Reductive Elimination Reactions in Gold(III) Complexes Leading to C(sp^3)–X (X = C, N, P, O, Halogen) Bond Formation: Inner-Sphere *vs* S_N2 Pathways

Alejandro Portugués,[a] *Miguel Ángel Martínez-Nortes*,[a] *Delia Bautista*,[b] *Pablo González-Herrero*,[a] *Juan Gil-Rubio**[a]

[a] Departamento de Química Inorgánica. Facultad de Química. Universidad de Murcia. Campus de Espinardo, 30100 Murcia (Spain). E-mail: jgr@um.es.

[b] ACTI, Universidad de Murcia. Campus de Espinardo, 30100 Murcia (Spain).

Abstract

The reactions leading to formation of C–heteroatom bonds in the coordination sphere of Au(III) complexes are uncommon and their mechanisms are not well known. This work reports on the synthesis and reductive elimination reactions of a series of Au(III) methyl complexes containing different Au–heteroatom bonds. Complexes [Au(CF_3)(Me)(X)(PR_3)] (R = Ph, X = OTf, $OClO_3$,

ONO_2, $OC(O)CF_3$, F, Cl, Br; R = Cy, X = Me, OTf, Br) were obtained by reaction of *trans*-$[Au(CF_3)(Me)_2(PR_3)]$ (R = Ph, Cy) with HX. The cationic complex *cis*-$[Au(CF_3)(Me)(PPh_3)_2]OTf$ was obtained by reaction of $[Au(CF_3)(Me)(OTf)(PPh_3)]$ with PPh_3. Heating these complexes led to reductive elimination of MeX (X = Me, Ph_3P^+, OTf, $OClO_3$, ONO_2, $OC(O)CF_3$, F, Cl, Br). Mechanistic studies indicate that these reductive elimination reactions occur either through (a) formation of tricoordinate intermediates by phosphine dissociation, followed by reductive elimination of MeX, or (b) attack of weakly-coordinating anionic (TfO^- or ClO_4^-) or neutral nucleophiles (PPh_3 or NEt_3) to the Au-bound methyl carbon. The obtained results show for the first time that nucleophilic substitution should be considered as a likely reductive elimination pathway in Au(III) alkyl complexes.

Introduction

The advances in the field of Au(I)/Au(III) catalysis during the last decade[1–15] have boosted research on fundamental aspects of gold redox reactions.[16–23] Thus, the oxidative addition of substrates containing C–Halogen, C–N_2^+ or strained C–C bonds to Au(I) complexes, regarded as the most challenging step of these catalytic cycles, has received considerable attention.[24–30] By contrast, reductive eliminations in Au(III) complexes have been less studied, despite the fact that the degree of selectivity in this step dramatically affects the outcome of the catalytic processes.[31] Pioneering studies carried out during the 1970's[32–34] revealed that reductive elimination in square planar Au(III) complexes can occur (a) through tricoordinate intermediates formed after ligand dissociation or (b) directly from the tetracoordinate complexes (Scheme 1, A).[24,25] Alternatively, a concerted mechanism where C–C and B–F bonds form simultaneously has been proposed for the reaction of Au(III) alkyl fluorido complexes with arylboronic acids (Scheme 1, B).[35] Whereas

the experimental evidence of pathways (a)[32–34,36–39] and (b)[35,40–48] is abundant for C–C coupling reactions, mechanistic data on reductive eliminations processes leading to C–heteroatom bond formation are scarce. The available information has been obtained on dissociative reductive eliminations of alkyl,[49,50] aryl,[38,51] or trifluoromethyl halides[52] and non-dissociative reductive eliminations of ArX derivatives (X = NR_2, PR_3^+, OR, SR, halogen).[53–59]

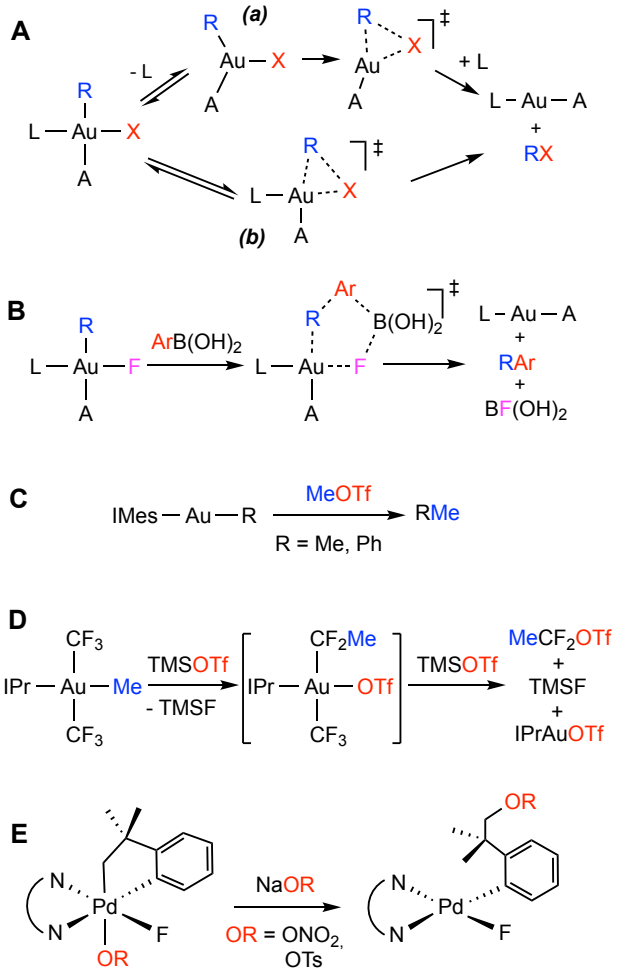

Scheme 1. (A) and (B) Reductive elimination pathways in square-planar Au(III) complexes. (C) Alkylation of methyl or aryl Au(I) complexes with MeOTf. (D and E) Reported reductive eliminations of organic esters of strong oxoacids. IMes = 1,3-dimesityl-1-H-imidazolydene; IPr = 1,3-bis(2,6-diisopropylphenyl)-1-H-imidazolydene.

Alkyl esters of strong oxyacids such as triflic, perchloric or nitric acids, are powerful electrophiles, capable of alkylating organic[60–62] or metal-based[63–66] nucleophiles. In particular, an oxidative addition of MeOTf has been invoked to explain the formation of ethane or toluene in the reaction of [AuR(IMes)] with MeOTf (Scheme 1, C).[67] The reverse reaction, namely the reductive elimination of organic triflates, perchlorates or nitrates from metal complexes is thus very unlikely. Nevertheless, it has been postulated for the Bi- or Cu-catalysed formation of aryl or vinyl triflates[68,69] and in the reaction of $[Au(CF_3)_2(Me)(IPr)]$ with Me_3SiOTf (Scheme 1, D).[70] Direct reductive elimination of an alkyl nitrate or tosylate has been observed in cyclometalated Pd(IV) complexes (Scheme 1, E).[71]

Herein we report a study on reductive elimination reactions from Au(III) complexes of the type $[Au(CF_3)(Me)X(PR_3)]$, which lead to C–C, C–N, C–P, C–O or C–halogen bond formation. Uncommon reductive elimination products, such as methyl fluoride, triflate, perchlorate and nitrate have been observed. Mechanistic and computational studies show that, depending on the ligand X, the classical dissociative pathway or an S_N2-type pathway operate in these reactions.

Results and discussion

Synthesis of Au(III) complexes. Bromination of $[Au(CF_3)(PR_3)]$ (R = Ph (**1a**), Cy (**1b**)) followed by reaction of the resulting dibromo complexes *trans*-$[AuBr_2(CF_3)(PR_3)]$ (R = Ph (**2a**), Cy (**2b**)) with methylmagnesium bromide afforded *trans*-$[Au(CF_3)(Me)_2(PR_3)]$ (R = Ph (**3a**), Cy (**3b**)) in good yields (Scheme 2), which are stable at room temperature under ambient light.

Complex **3a** rapidly reacted in chloroform or dichloromethane with strong protic acids, such as triflic, concentrated aqueous perchloric or nitric, trifluoroacetic, hydrobromic, or hydrochloric

acid to give methane and complexes [Au(CF_3)(Me)(X)(PPh_3)] (X = OTf (**4a**), $OClO_3$ (**5a**), ONO_2 (**6a**), $OC(O)CF_3$ (**7a**), Br (**8a**), Cl (**9a**)), as the main reaction products (Scheme 2). Similarly, the reaction of **3b** with triflic or hydrobromic acid gave [Au(CF_3)(Me)(X)(PCy_3)] (X = OTf (**4b**), Br (**8b**)). Remarkably, only one of the methyl ligands was protonated, even in the presence of an excess of acid. No significant reaction was observed between **3a** and hydrofluoric acid, acetic acid, phenol or 4-methoxythiophenol. The protonation of the robust Au–C(sp^3) bonds[72] of **3a** or **3b** with acids is in line with the previous results of Kochi and co-workers on the protonolysis of complexes [Au(alkyl)$_3$(phosphine)],[36] where only one of the Au–alkyl bonds *cis* to the phosphine is protonated, in agreement with the mutually exerted large *trans* effect of these alkyl ligands.

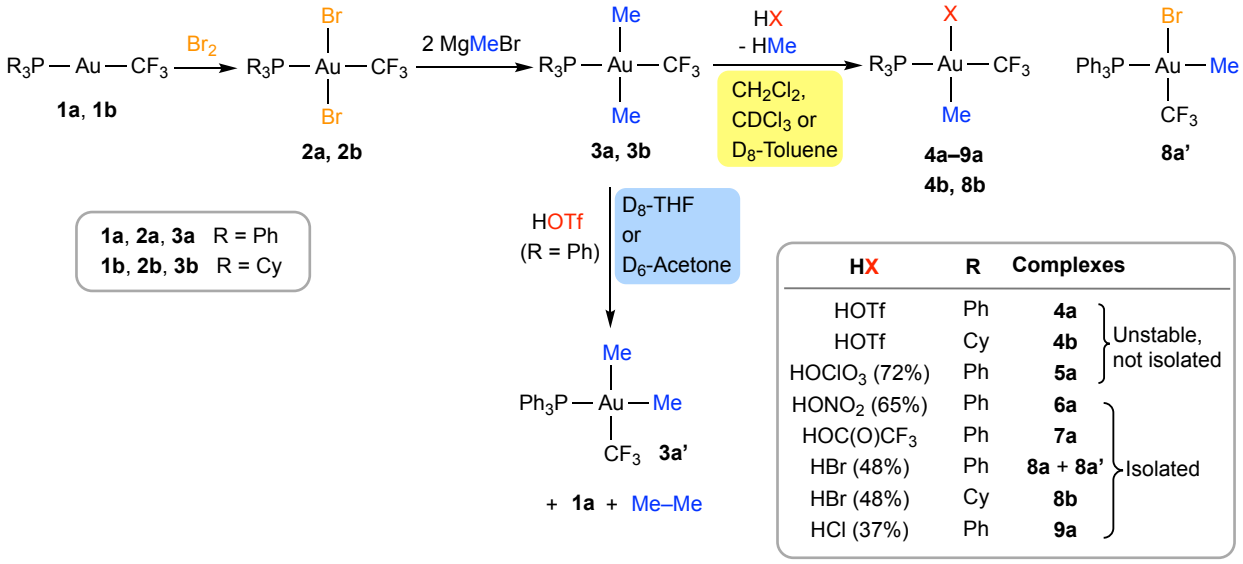

Scheme 2. Synthesis and reactions with acids of Au(III) methyl complexes.

Complexes **6a**, **7a**, **8a** and **8b** were isolated in good yields. The isolated samples of **8a** contained small amounts (4–7%) of the corresponding isomer **8a'**, where the PPh_3 and Me ligands are

mutually *trans* (see below). In contrast, the attempts to isolate **4a**, **4b** or **5a** gave impure oils, which we attribute to their lower stabilities (see Supporting Information).

The outcome of the reaction of **3a** with triflic acid depended on the solvent. Thus, the Au–Me bond acidolysis was the dominant process in dichloromethane, chloroform or toluene, whereas the isomerization to *cis*-[Au(CF_3)($Me)_2$(PPh_3)] (**3a'**), with concurrent reductive elimination of ethane, was the main process in THF or acetone (Scheme 2). This reaction occurs even in the presence of a substoichiometric amount of acid (10%), but not when acetic acid was used instead of triflic acid.

These observations can be rationalized by considering the influence of the solvent on the pK_a of triflic acid.[73] Thus, the irreversible Au–Me acidolysis needs a strongly acidic medium and therefore it takes place only in those solvents where the pK_a of the acid is lowest (dichloromethane, chloroform and toluene). In contrast, in THF or acetone the pK_a of triflic acid would not be low enough to protonate the methyl carbon. Then, other reaction pathways would come into play, where the acidic medium facilitates the isomerization and reductive elimination reactions of the Au(III) complexes (see below).

The reaction of a mixture of isomers **8a** and **8a'** with AgF gave AgBr and the corresponding fluorido complexes **10a** and **10a'** (Scheme 3), which were unambiguously identified in solution by NMR spectroscopy, but could not be isolated in pure form. The reaction of *in situ*-generated **4a** and KI gave a mixture containing mainly PPh_3, [Au(CF_3)(Me)(I)(PPh_3)] (**11a** and **11a'**) and another gold complex containing the CF_3 and CH_3 ligands, but lacking the PPh_3 ligand, which was tentatively identified as *cis*- or *trans*-K[Au(CF_3)(Me)I_2] (**12**) (Scheme 3). MeI and [AuI(PPh_3)] were also detected by NMR spectroscopy in the reaction mixture. The reaction of **4a**

with PPh_3 cleanly gave *cis*-[Au(CF_3)(Me)(PPh_3)$_2$] (**13**), which was isolated in good yield (Scheme 3).

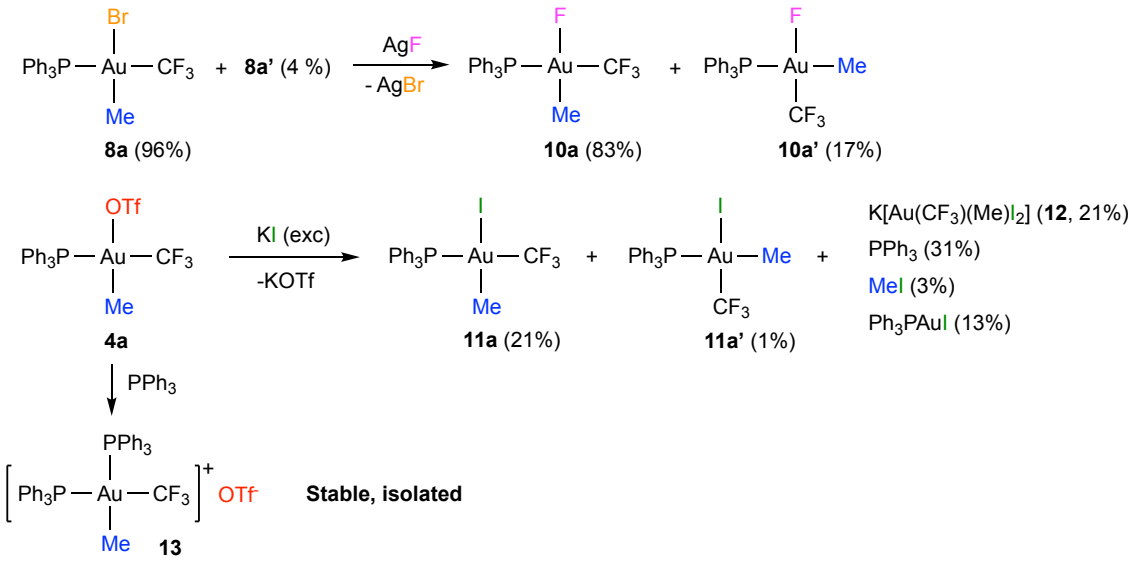

Scheme 3. Synthesis of Au(III) fluorido, iodido and cationic bis(phosphine) complexes.

Single crystals were obtained from an *in situ*-generated solution of **5a**. However, the X-ray diffraction analysis showed that the crystal contained the salt [Au(CF_3)(Me)(OH_2)(PPh_3)]ClO_4 (**5a**·H_2O), instead of the expected perchlorato complex (Figure 1), suggesting that under the reaction conditions, **5a** and H_2O are in equilibrium with **5a**·H_2O. In the crystal structure, each ClO_4^- anion is hydrogen-bonded to two coordinated water molecules to form ···O–Cl–O···H–O–H··· chains along the *a* axis. The Au–OH_2 distance (2.1562(17) Å) is almost identical to the value found in *cis*-[Au(Me)$_2$(OTf)(OH_2)] (2.157(6) Å).[74] The crystal structure of **6a** (Figure 1) shows that the nitrato ligand is coordinated to gold through one of the oxygen atoms. The Au–ONO_2 distance (2.133(2) Å) is similar to that found in [Au(CH_2COMe)(ONO_2)(ppy)] (2.128(3) Å; ppy

= 2-phenylen-2'-yl-pyridine),[75] but longer than in $[Au(CF_3)_3(ONO_2)]$ (2.090(4) Å).[76] In both **5a**·H_2O and **6a**, the trifluoromethyl and phosphine ligands are in a mutual *trans* disposition.

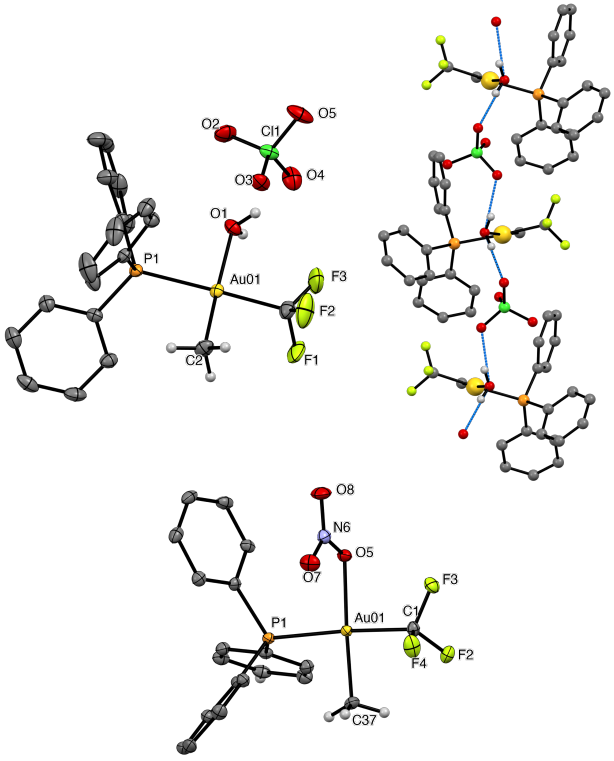

Figure 1. ORTEP representations (50% ellipsoids, phenylic H's omitted) of the structures of the cation and the anion of the salt $[Au(OH_2)(CF_3)(Me)(PPh_3)]ClO_4$ (**5a**·H_2O) (up, left) and complex **6a** (down). Representation of the chains of ···H–O–H···O–Cl–O··· hydrogen bonds between the ClO_4^- anions and H_2O ligands of the salt (up, right). Tables of bond lengths and angles are included in the Supporting Information.

The ^{19}F and $^{31}P\{^1H\}$ NMR spectra of **3a–9a**, **11a**, **3b**, **4b** and **8b** showed a doublet and a quartet, respectively, with a large $^3J_{PF}$ value (62.4–72.8 Hz) characteristic of a mutually *trans* arrangement of the phosphine and trifluoromethyl ligands. The $^{31}P\{^1H\}$ NMR spectrum of **13**

showed the presence of two inequivalent and mutually coupled ^{31}P nuclei with an additional splitting due to ^{31}P-^{19}F coupling, indicating a *cis* configuration. The $^{19}F_3C$ and $^{31}PPh_3$ resonances of **10a** and **10a'** show coupling with the gold-bound fluorine nucleus, and the ^{19}F-NMR spectrum of the mixture displays two signals at -223.7 (**10a**) and -246.6 ppm (**10a'**), which fall in the same region as those of previously reported Au(III) fluorido complexes.[49,77,78]

Reductive elimination and isomerization reactions. Heating of solutions of the Au(III) complexes led to reductive elimination of MeX (X = Me, OTf, $OClO_3$, ONO_2, $OC(O)CF_3$, F, Cl, Br) as the major process, with formation of $[Au(CF_3)(PR_3)]$ (R = Ph (**1a**) or Cy (**1b**)) (Scheme 4 and Table 1). Thermal isomerization was observed as a secondary process in most cases. Upon heating, the concentration of isomers **5a'**–**10a'** increased rapidly and then remained steady at the equilibrium proportions shown in Table 1, until both isomers completely transformed into the corresponding reductive elimination products. Exceptions to this behaviour were the triflato complex **4a**, which gave very small amounts of its isomer **4a'**, and the PCy_3 complexes **3b**, **4b** and **8b**, for which no isomerization was observed. The fastest decompositions were observed for the triflato and perchlorato complexes (**4a**, **4b** and **5a**), which were consumed in 0.5–4.5 h at 50 °C. In contrast, the decomposition of **6a**, **7a**, **8a**, **9a** or **10a** required higher temperatures and longer times. Finally, the decomposition of the PCy_3 complexes **3b** and **8b** required more energetic conditions compared to their PPh_3 counterparts **3a** and **8a**.

Au(I) complexes $[Au(PR_3)_2]^+$ (R = Ph or Cy) were formed as secondary products in most cases. These products arise from hydrolysis or decomposition of the resulting Au(I) complexes **1a** and **1b** (see Supporting Information). Small amounts (5%) of phosphonium salts $(PMePh_3)X$ (X = $OC(O)CF_3$, Cl, Br) were observed in the decompositions of **7a**, **8a** and **9a**. Similarly, complex **13**

underwent a quantitative reductive elimination of $(PMePh_3)OTf$ after heating for 2 h at 80 °C, or 4 h at 60 °C (Scheme 4).

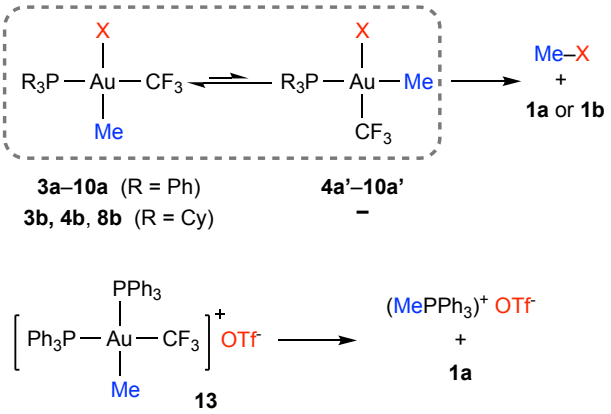

Scheme 4. Thermal decomposition and isomerization of the Au(III) complexes.

Table 1. Decomposition of the Au(III) complexes: reaction temperatures and times, isomerization degree, and observed secondary products.[a]

Complexes	X	T (°C)	t (h)[b]	Isom. %[c]	MeX yield (%)[f]	Secondary products
3a	Me	100	27	–	> 95[g]	–
3b	Me	140	> 14[e]	–	–	–
4a, **4a'**[d]	OTf	50	3.5	< 4	70	$[Au(PPh_3)_2]X$, Au
4b[d]	OTf	50	4.5	–	70	$[Au(PCy_3)_2]X$, $[AuX(PCy_3)]$, Au
5a, **5a'**[d]	$OClO_3$	50	0.5	5	50	$[Au(PPh_3)_2]X$, Au
6a, **6a'**	ONO_2	80	6	12	78	$[Au(PPh_3)_2]X$, Au, unknown
7a, **7a'**	$OCOCF_3$	100	17.5	20	83[g]	$(PMePh_3)X$ (5%)
10a, **10a'**	F	110	14	17	–[h]	$[Au(PPh_3)_2]X$, ethane
9a, **9a'**	Cl	80	5	16	–[h]	Ph_3PAuCl, $(PMePh_3)Cl$

						(5%)
8a, **8a'**	Br	80	4.3	18	79[g]	Ph_3PAuBr, $(PMePh_3)Br$ (5%)
8b	Br	110	20	–	–[h]	–

[a] All experiments were carried out in $CDCl_3$ except the decompositions of **3a**, **3b** and **7a**, which were carried out in D_8-toluene (all spectra are given in the Supporting Information). [b] Necessary time for consumption of at least 95% of the starting Au(III) complex. [c] Equilibrium proportion of isomers **4a'**–**10a'**. [d] *In situ* generated from **3a** or **3b** and HX. [e] The conversion was 6.6% after 14 h. [f] Determined by integration of the ^1H NMR spectra measured before and after the reaction. [g] Indirectly estimated from the resulting concentration of **1a**. [h] The yield was not accurately determined in these cases.

The configurational assignment of isomers **3a'**–**11a'** is supported by their smaller $^3J_{PFcis}$ (9.1–11.8 Hz) and larger $^3J_{PHtrans}$ (8.9–9.7 Hz) values with respect to those of **3a**–**11a** ($^3J_{PFtrans}$ 62.4–72.8 Hz; $^3J_{PHcis}$ 5.8–6.6 Hz), as well as by the larger ^{31}P-$^{13}CH_3$ coupling constant of **7a'** ($^2J_{PCtrans}$ = 91.6 Hz) compared to that of **7a** ($^2J_{PCcis}$ = 3.8 Hz).[79]

Mechanistic studies. The concentrations of the reactants and products during the thermal decomposition of representative complexes (**3a**, **8a**, and **13**) were monitored by NMR spectroscopy. In addition, the effect of the presence of an additional amount of PPh_3 was studied.

The decomposition of the dimethyl complex **3a** was monitored at 100 °C (Figure 2). The formation of ethane from **3a** was drastically inhibited by the addition of PPh_3 (0.2 or 1 equiv), which is in agreement with a mechanism where PPh_3 dissociation gives the tricoordinate intermediate $[Au(CF_3)(Me)_2]$, which decomposes to give ethane (Scheme 5). Remarkably, the rate of consumption of **3a** increased with time until approximately half conversion, suggesting acceleration of the reaction by one of the reaction products. Indeed, the reaction was faster in the presence of added **1a** (Figure 2). The exchange between coordinated and free PPh_3 in a sample containing **1a** and PPh_3 was observed, in agreement with **1a** and PPh_3 being in equilibrium with

[$Au(CF_3)(PPh_3)_2$] (see Figures S86 and S103). This would decrease the concentration of free PPh_3, increasing the amount of the tricoordinate intermediate (Scheme 5).

The proposed dissociative mechanism also explains the observed catalytic effect of triflic acid on the decomposition and isomerization of **3a** to **3a'** in acetone or THF. Thus, protonation of free PPh_3 would shift the phosphine-dissociation equilibrium toward the tricoordinate intermediate at room temperature (Scheme 5). This intermediate could undergo elimination of ethane or coordinate a molecule of PPh_3 to give **3a'**. In the absence of acid, achieving a significant PPh_3 dissociation degree would require a higher temperature, which would produce the decomposition of the tricoordinate intermediate to give ethane and **1a**.

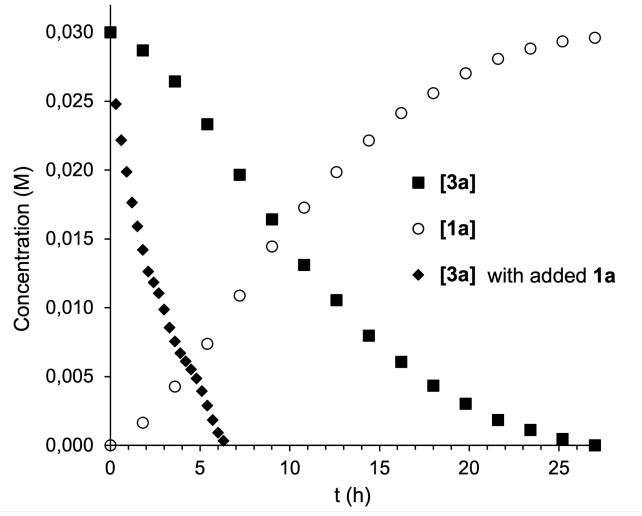

Figure. 2. Thermal decomposition of **3a** (100 °C, D_8-Toluene): [**3a**] and [**1a**] *vs*. time; [**3a**] *vs*. time in the presence of added **1a** (4.6 equiv). Concentrations were determined by integration of the ^{19}F NMR spectra using $PhCF_3$ as internal standard.

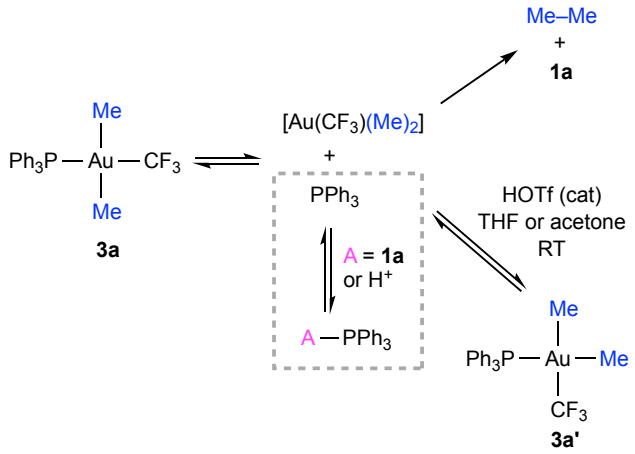

Scheme 5. Proposed dissociative mechanism for the decomposition and isomerization of **3a**. Effect of **1a** or HOTf on the PPh_3 dissociation equilibrium.

Heating of a solution of the bromido complexes **8a** (96%) and **8a'** (4%) at 80 °C led to rapid equilibration of both isomers at a 82:18 ratio, respectively, which remained constant during the reaction (Figure 3). As observed for **3a**, the rate of formation of **1a** increased with time until half conversion, suggesting acceleration of the reaction by a reaction product. In the presence of one additional equivalent of PPh_3, both the consumption of **8a** and **8a'** and the formation of MeBr were slower, in agreement with a PPh_3-dissociative pathway (Figure S83). However, in these conditions the major reaction product was $(PMePh_3)Br$ (Scheme 6). Similarly, heating of $[Au(CF_3)(Me)(Cl)(PPh_3)]$ (**9a**) in the presence of PPh_3 (5 equiv) gave mainly $(PMePh_3)Cl$.

The slower reductive eliminations of the tricyclohexylphosphine complexes **3b** and **8b** are also in line with phosphine dissociation being the rate-determining step, and are attributed to the higher donor-ability of PCy_3 compared with PPh_3.

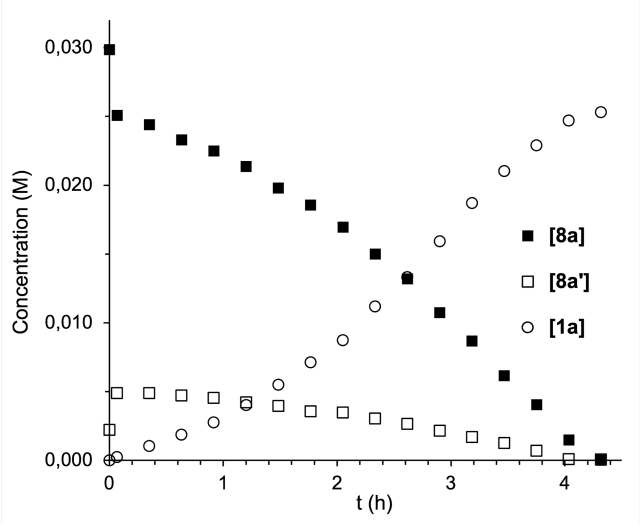

Figure. 3. [**8a**], [**8a'**] and [**1a**] *vs*. time (80 °C, $CDCl_3$). Concentrations were determined by integration of the ^{19}F NMR spectra using $PhCF_3$ as internal standard.

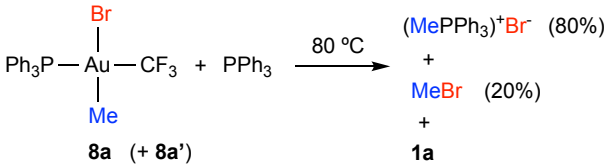

Scheme 6. Decomposition of **8a** and **8a'** in the presence of added PPh_3.

The decomposition of **13** into **1a** and $(PMePh_3)OTf$ was monitored at 60 °C in $CDCl_3$ (Figure 4). In marked contrast with the behaviour of **3a** and **8a**, the depletion of **13** showed a first-order dependence until an 85% conversion and, importantly, was accelerated by added PPh_3 (the completion time decreased from 4 to 0.25 h in the presence of 5 equiv of PPh_3). Since this PPh_3-induced reaction acceleration is not compatible with a phosphine-dissociative mechanism, concerted reductive elimination from a pentacoordinate intermediate or nucleophilic attack of PPh_3 on the methylic carbon were considered as alternative pathways.

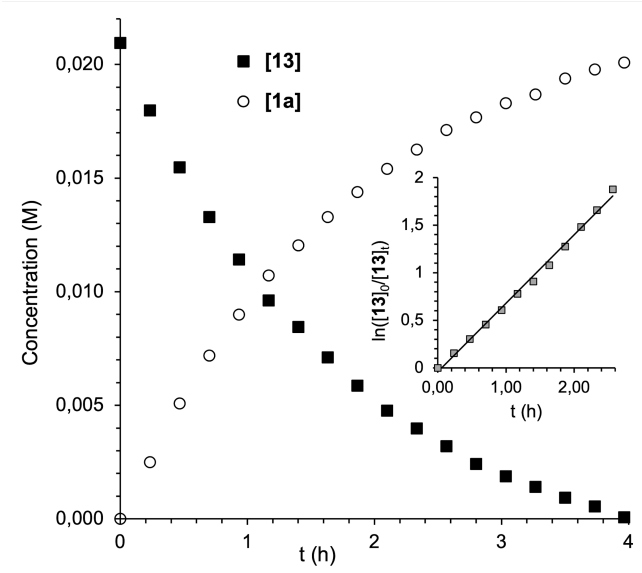

Figure. 4. Thermal decomposition of **13** (60 °C in $CDCl_3$): [**13**] and [**1a**] *vs*. time; (insert) plot of $\ln([\mathbf{13}]_0/[\mathbf{13}]_t)$ *vs*. time illustrating the first order decay of [**13**] up to a conversion of 85% (t = 2.57 h). Concentrations were determined by integration of the ^{19}F NMR spectra using $PhCF_3$ as internal standard.

The room-temperature ^{31}P NMR spectrum of a mixture of **13** and PPh_3 did not show evidence of pentacoordinated species. Instead, only three sharp signals corresponding to **13** and free PPh_3 were observed (Figure S103). To test the possibility of a nucleophilic attack, **13** was reacted with 2 equivalents of NEt_3 at 50 °C. In these conditions, **1a** and a mixture of $(PMePh_3)OTf$ and $(NEt_3Me)OTf$ in a 0.78 to 1 molar ratio was formed (Scheme 7, *(a)*). Besides, no signs of NEt_3 coordination, or substitution of PPh_3 by NEt_3 were found in the NMR spectra. Overall, these observations point to external attack of PPh_3 or NEt_3 on the methyl carbon being the main reaction pathway.

In the absence of added phosphine, the formation of $(PMePh_3)OTf$ from **13** could possibly occur through the dissociation of PPh_3 followed by nucleophilic substitution on the methyl

carbon (Scheme 7, *(b)*). In agreement with this, reductive elimination of phosphonium salt was faster in solvents with a higher coordinating ability (reaction times at 60 °C: 1.5 h in acetone, 0.75 h in acetonitrile). The fast dissociation of PPh_3 was evidenced by the $^{31}P\{^1H\}$ NMR spectrum of **13** at 60 °C as a broadening of the signal of the ^{31}P *trans* to the methyl ligand, with loss of P-P and P-F couplings (Figure S100). In addition, the observed first-order dependence of the consumption rate of **13** agrees with this mechanism, if a steady concentration of the intermediate is assumed (Figure S96).

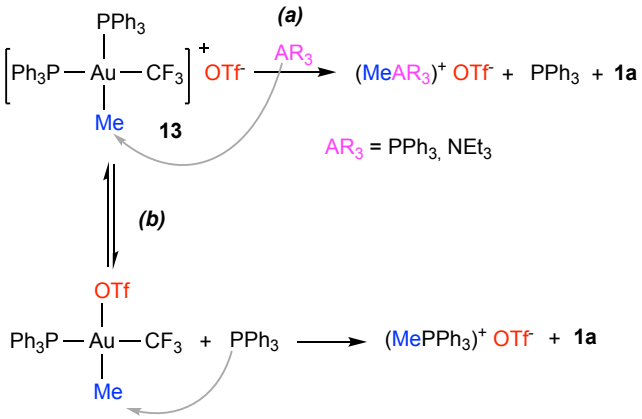

Scheme 7. Nucleophilic attack on the methyl carbon of (a) added PPh_3 or NEt_3, (b) dissociated PPh_3.

The formation of $(PMePh_3)X$ (X = Cl, Br) from **8a** or **9a** in the presence of PPh_3 could follow a similar pathway, although in this case a fraction of the observed phosphonium salts could be originated by the reaction of the formed MeBr or MeCl with PPh_3. Formation of small amounts of phosphonium salts during the thermal decompositions of **7a**, **8a** and **9a** (Table 1) suggests that the S_N2 pathway could be a secondary reductive elimination route in these cases.

The conversion of complexes **6a**, **7a**, **9a** or **10a** into **1a** and $MeONO_2$, $MeOC(O)CF_3$, MeCl or MeF, respectively, needed reaction times (5–20 h) and temperatures (80–100 °C) comparable to those of **8a**. The equilibrium amount of their respective isomers **6a'**, **7a'**, **9a'** or **10a'** (12–20%)

was similar to that of **8a'** (18%). Considering these similarities, we propose that they mainly proceed through a phosphine-dissociative mechanism similar to that of **8a**.

In marked contrast, the reductive eliminations of MeOTf or $MeOClO_3$ from **4a**, **4b** or **5a** were significantly faster, suggesting a different reaction pathway. In addition, complexes **4a** and **4b** show comparable decomposition times, meaning that phosphine dissociation is not rate-determining in these cases. Considering the low coordinating abilities of OTf^- and ClO_4^-, the degree of anion dissociation is expected to be higher for **4a**, **4b** or **5a** compared with the rest of studied complexes, and thus could reasonably be the starting point of the observed reactivity.

Computational study. For an understanding of the decomposition reactions of the Au(III) complexes bearing a labile anionic ligand, the reductive elimination of MeOTf from **4a** was modelled using DFT calculations at the B3LYP/(6-31G**+LANL2DZ) level in chloroform solution (see details in the Supporting Information). Different pathways involving the dissociation of PPh_3 or OTf^- as the first step were calculated and compared (Figure 5). In both cases, the relaxed scan of the potential energy as the Au-P or Au-O distance was elongated to 4.5 or 3.2 Å, respectively, resulted in a Morse-type curve with a gradual increase in energy as the ligands are separated from the metal (Figure S110). Therefore, no transition state can be located using this theoretical model. These scans appear to indicate a higher activation barrier for the dissociation of PPh_3 compared to that of OTf^-. However, the calculated free energy change for the dissociation of OTf^- to give the cationic tricoordinate intermediate $[Au(CF_3)(Me)(PPh_3)]^+$ (**Int1$^+$**) is significantly higher relative to the dissociation of PPh_3 to give $[Au(CF_3)(Me)(OTf)]$ (**Int2**), the latter being slightly exergonic. This can be explained by a higher entropy increase upon dissociation of PPh_3 and, more importantly, an additional stabilization of the **Int2** fragment due to the chelating coordination of the OTf^- ligand.

The C–O coupling step could occur from **Int1**$^+$ through two different mechanisms. The first one involves a three-centered transition state with a pseudotetrahedral coordination around the gold atom (**TS1A**), having a very high free energy. The second one involves an S_N2-like transition state resulting from the nucleophilic attack of the OTf^- anion on the methyl ligand (**TS1B**) and provides a much more favourable pathway because it has virtually the same free energy as the previous dissociation step. On the other hand, the C–O coupling from **Int2** would occur through a highly energetic tricoordinate transition state (**TS2**), which makes the PPh_3 dissociation pathway clearly unfavourable. The attempts to model concerted reaction pathways through pseudotetrahedral or planar transition states formed from **4a** or **4a'**, respectively converged to a transition state very similar to **TS1A**.

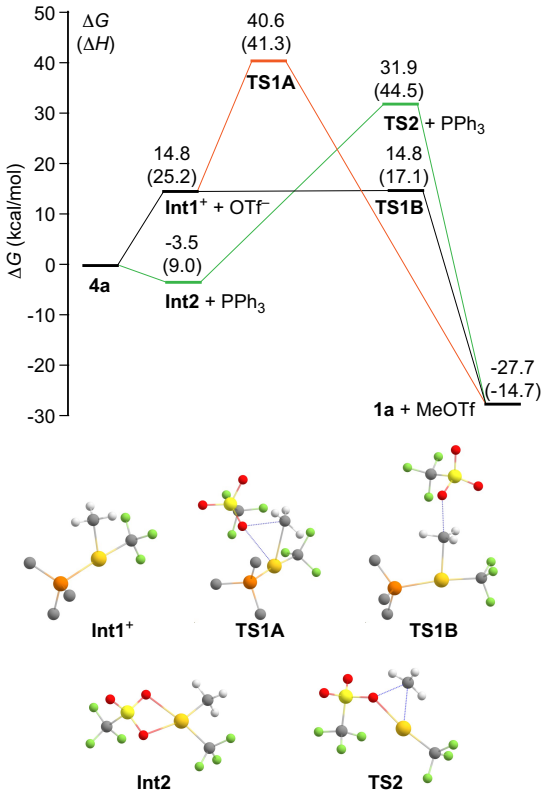

Figure 5. Free-energy profiles (in kcal/mol) of the modelled reaction pathways for the reductive elimination of MeOTf from complex **4a** and structures of intermediate species and transition states. Enthalpies are given in parentheses.

Thus, on the basis of these calculations and the above presented experimental data, the C–O reductive couplings from **4a**, **4b** or **5a** occur most likely via dissociation of the labile anionic ligand and subsequent nucleophilic attack on the metal-bound methyl group (Scheme 8). Previous studies have revealed that this is a feasible pathway for the reductive elimination of Csp^3–X (X = N, O, Cl, Br, I) coupling products in Rh(III),[80,81] Pd(II),[82] Pd(IV)[71,83,84] and Pt(IV)[85–88] alkyl complexes. Interestingly, the studies on Pt(IV) complexes showed that reductive elimination is faster for more electron-deficient anions,[86] despite their lower nucleophilicity.[89] The S_N2 reductive elimination mechanism has been previously considered for Au(III) complexes, but to the best of our knowledge, no experimental evidence has been provided. Thus, in a computational study of the Au-catalized methane oxidation, Periana and co-workers proposed that formation of the O–CH_3 bond could take place through nucleophilic attack of a free HSO_4^- anion on an intermediate Au(III) methyl complex.[90] Later, Bercaw and co-workers discarded a S_N2-type pathway for the reductive elimination of MeI from [Au(Me)$(I)_2$(IPr)].[50]

The lowest unoccupied molecular orbital (LUMO) isosurface of **Int1**$^+$ (Figure 6) provides additional support for the proposed mechanism. It is a σ* orbital mostly distributed along the Au–C bond, with large external lobes, implying that both the C and Au atoms can display Lewis-acidic behaviour. The electrophilicity of the Me group in this species is also supported by the above discussed nucleophilic attacks of PPh_3 or NEt_3 on this group.

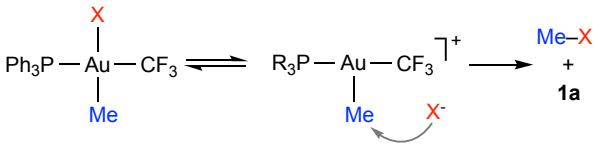

Scheme 8. Decomposition of triflate or perchlorate complexes by anion dissociation followed by nucleophilic attack.

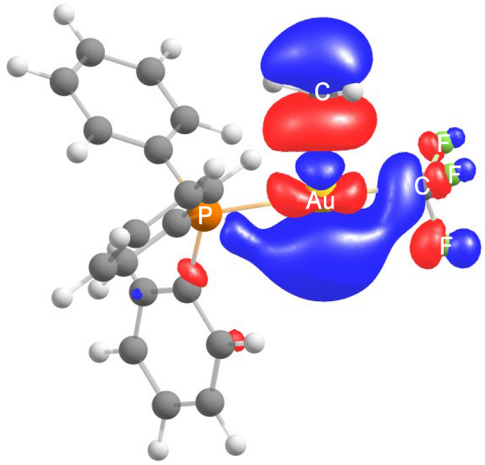

Figure 6. LUMO isosurface (0.035 e bohr^{-3}) for the cationic species **Int1**$^{+}$.

Conclusions

The thermal decomposition of complexes [Au(CF_3)(Me)(X)(PR_3)] leads to [Au(CF_3)(PR_3)] and C(sp^3)–X (X = C, P, O, F, Cl, Br) coupling products. The observed reactions include rare examples of reductive eliminations of methyl fluoride or highly electrophilic molecules such as methyl triflate or perchlorate. Reductive elimination is accompanied by partial isomerization of the corresponding Au(III) complexes.

Mechanistic studies indicate that the reductive eliminations of ethane or methyl bromide from [Au(CF_3)(Me)(X)(PR_3)] (X = Me, Br) take place from a tricoordinate intermediate formed by phosphine dissociation. In contrast, in the cases of the analogous complexes with X = OTf or ClO_4, and the cationic complex *cis*-[Au(CF_3)(Me)(PPh_3)$_2$]OTf, experimental evidence and computational modelling are consistent with a reaction pathway involving X^- or PPh_3 dissociation followed by nucleophilic attack to the gold-bound carbon. This S_N2 reductive elimination mechanism has not been documented before in Au(III) complexes and therefore should be considered as a potential pathway in Au(I)/Au(III) catalysed reactions, in particular in those leading to C(sp^3)–X coupling products.

Associated Content

Supporting Information. Synthetic procedures, characterization data, NMR spectra, decomposition and mechanistic experiments, crystallographic data, details of the computational study (PDF).

Accesion Codes. CCDC 2214042 and 2214043 contain the supplementary crystallographic data for this paper. These data can be obtained free of charge via www.ccdc.cam.ac.uk/data_request/cif, or by emailing data_request@ccdc.cam.ac.uk, or by contacting The Cambridge Crystallographic Data Centre, 12 Union Road, Cambridge CB2 1EZ, UK; fax: +44 1223 336033.

Notes. The authors declare no competing finantial interest.

Acknowledgements

Financial support from the following grants is gratefully acknowledged: Grant PGC2018-100719-B-I00 funded by MCIN/AEI/ 10.13039/501100011033 and by ERDF A way of making Europe; Grant 19890/GERM/15 funded by Séneca Foundation of the Region of Murcia (Ayudas a Grupos de Excelencia).

References

(1) Nijamudheen, A.; Datta, A. Gold-Catalyzed Cross-Coupling Reactions: An Overview of Design Strategies, Mechanistic Studies, and Applications. *Chem. Eur. J.* **2020**, *26*, 1442–1487.

(2) Hopkinson, M. N.; Gee, A. D.; Gouverneur, V. Au^{I}/Au^{III} Catalysis: An Alternative Approach for C-C Oxidative Coupling. *Chem. Eur. J.* **2011**, *17*, 8248–8262.

(3) Wegner, H. A.; Auzias, M. Gold for C-C Coupling Reactions: A Swiss-Army-Knife Catalyst? *Angew. Chem. Int. Ed.* **2011**, *50*, 8236–8247.

(4) Fricke, C.; Reid, W. B.; Schoenebeck, F. A Review on Oxidative Gold-Catalyzed C-H Arylation of Arenes – Challenges and Opportunities. *Eur. J. Org. Chem.* **2020**, 7119–7130.

(5) Zheng, Z.; Ma, X.; Cheng, X.; Zhao, K.; Gutman, K.; Li, T.; Zhang, L. Homogeneous Gold-Catalyzed Oxidation Reactions. *Chem. Rev.* **2021**, *121*, 8979–9038.

(6) Witzel, S.; Hashmi, A. S. K.; Xie, J. Light in Gold Catalysis. *Chem. Rev.* **2021**, *121*, 8868–8925.

(7) Akram, M. O.; Banerjee, S.; Saswade, S. S.; Bedi, V.; Patil, N. T. Oxidant-Free Oxidative Gold Catalysis: The New Paradigm in Cross-Coupling Reactions. *Chem. Commun.* **2018**,

54, 11069–11083.

(8) Bhoyare, V. W.; Tathe, A. G.; Das, A.; Chintawar, C. C.; Patil, N. T. The Interplay of Carbophilic Activation and Au(I)/Au(III) Catalysis: An Emerging Technique for 1,2-Difunctionalization of C–C Multiple Bonds. *Chem. Soc. Rev.* **2021**, *50*, 10422–10450.

(9) Han, C.; Liu, Y.; Tian, X.; Rominger, F.; Hashmi, A. S. K. Dual Gold/Silver Catalysis: Indolizines from 2-Substituted Pyridine Derivatives via a Tandem C(sp^3)–H Alkynylation/Iminoauration. *Org. Lett.* **2021**, *23*, 9480–9484.

(10) Rigoulet, M.; Thillaye du Boullay, O.; Amgoune, A.; Bourissou, D. Gold(I)/Gold(III) Catalysis That Merges Oxidative Addition and π-Alkene Activation. *Angew. Chem. Int. Ed.* **2020**, *59*, 16625–16630.

(11) Rodriguez, J.; Adet, N.; Saffon-Merceron, N.; Bourissou, D. Au(I)/Au(III)-Catalyzed C–N Coupling. *Chem. Commun.* **2019**, *56*, 94–97.

(12) Yang, Y.; Schießl, J.; Zallouz, S.; Göker, V.; Gross, J.; Rudolph, M.; Rominger, F.; Hashmi, A. S. K. Gold-Catalyzed C(sp^2)–C(sp) Coupling by Alkynylation through Oxidative Addition of Bromoalkynes. *Chem. Eur. J.* **2019**, *25*, 9624–9628.

(13) Yang, Y.; Antoni, P.; Zimmer, M.; Sekine, K.; Mulks, F. F.; Hu, L.; Zhang, L.; Rudolph, M.; Rominger, F.; Hashmi, A. S. K. Dual Gold/Silver Catalysis Involving Alkynylgold(III) Intermediates Formed by Oxidative Addition and Silver-Catalyzed C–H Activation for the Direct Alkynylation of Cyclopropenes. *Angew. Chem. Int. Ed.* **2019**, *58*, 5129–5133.

(14) Liu, K.; Li, N.; Ning, Y.; Zhu, C.; Xie, J. Gold-Catalyzed Oxidative Biaryl Cross-

Coupling of Organometallics. *Chem* **2019**, *5*, 2718–2730.

(15) Liu, Y.; Dietl, M. C.; Han, C.; Rudolph, M.; Rominger, F.; Krämer, P.; Hashmi, A. S. K. Synthesis of Amide Enol 2-Iodobenzoates by the Regio- and Stereoselective Gold-Catalyzed Acyloxyalkynylation of Ynamides with Hypervalent Iodine Reagents. *Org. Lett.* **2022**, *24*, 7101–7106.

(16) Daley, R. A.; Morrenzin, A. S.; Neufeldt, S. R.; Topczewski, J. J. Mechanistic Investigation into the Gold-Catalyzed Decarboxylative Cross-Coupling of Iodoarenes. *ACS Catal.* **2021**, *11*, 9578–9587.

(17) Rodriguez, J.; Holmsen, M. S. M.; García-Rodeja, Y.; Sosa Carrizo, E. D.; Lavedan, P.; Mallet-Ladeira, S.; Miqueu, K.; Bourissou, D. Nucleophilic Addition to π-Allyl Gold(III) Complexes: Evidence for Direct and Undirect Paths. *J. Am. Chem. Soc.* **2021**, *143*, 11568–11581.

(18) Navarro, M.; Toledo, A.; Mallet-Ladeira, S.; Sosa Carrizo, E. D.; Miqueu, K.; Bourissou, D. Versatility and Adaptative Behaviour of the P^N Chelating Ligand MeDalphos within Gold(I) π Complexes. *Chem. Sci.* **2020**, *11*, 2750–2758.

(19) Rodriguez, J.; Szalóki, G.; Sosa Carrizo, E. D.; Saffon-Merceron, N.; Miqueu, K.; Bourissou, D. Gold(III) π-Allyl Complexes. *Angew. Chem. Int. Ed.* **2020**, *59*, 1511–1515.

(20) Genoux, A.; Biedrzycki, M.; Merino, E.; Rivera-Chao, E.; Linden, A.; Nevado, C. Synthesis and Characterization of Bidentate (P^N)Gold(III) Fluoride Complexes: Reactivity Platforms for Reductive Elimination Studies. *Angew. Chem. Int. Ed.* **2021**, *60*, 4164–4168.

(21) Kumar, R.; Krieger, J.-P.; Gómez-Bengoa, E.; Fox, T.; Linden, A.; Nevado, C. The First Gold(III) Formate: Evidence for β-Hydride Elimination. *Angew. Chem. Int. Ed.* **2017**, *56*, 12862–12865.

(22) Beucher, H.; Schörgenhumer, J.; Merino, E.; Nevado, C. Chelation-Assisted C–C Bond Activation of Biphenylene by Gold(I) Halides. *Chem. Sci.* **2021**, *12*, 15084–15089.

(23) González, J. A.; Verdugo, F.; Mascareñas, J. L.; López, F.; Nevado, C. [C^N]-Alkenyl Gold(III) Complexes by Proximal Ring-Opening of (2-Pyridyl)alkylidenecyclopropanes: Mechanistic Insights. *Angew. Chem. Int. Ed.* **2020**, *59*, 20049–20054.

(24) Joost, M.; Amgoune, A.; Bourissou, D. Reactivity of Gold Complexes towards Elementary Organometallic Reactions. *Angew. Chem. Int. Ed.* **2015**, *54*, 15022–15045.

(25) Rocchigiani, L.; Bochmann, M. Recent Advances in Gold(III) Chemistry: Structure, Bonding, Reactivity, and Role in Homogeneous Catalysis. *Chem. Rev.* **2021**, *121*, 8364–8451.

(26) Font, P.; Ribas, X. Fundamental Basis for Implementing Oxidant-Free Au(I)/Au(III) Catalysis. *Eur. J. Inorg. Chem.* **2021**, 2556–2569.

(27) Yang, Y.; Eberle, L.; Mulks, F. F.; Wunsch, J. F.; Zimmer, M.; Rominger, F.; Rudolph, M.; Hashmi, A. S. K. Trans Influence of Ligands on the Oxidation of Gold(I) Complexes. *J. Am. Chem. Soc.* **2019**, *141*, 17414–17420.

(28) Rodriguez, J.; Tabey, A.; Mallet-Ladeira, S.; Bourissou, D. Oxidative Additions of Alkynyl/Vinyl Iodides to Gold and Gold-Catalyzed Vinylation Reactions Triggered by the MeDalphos Ligand. *Chem. Sci.* **2021**, *12*, 7706–7712.

(29) Szalóki, G.; Babinot, J.; Martin-Diaconescu, V.; Mallet-Ladeira, S.; García-Rodeja, Y.; Miqueu, K.; Bourissou, D. Ligand-Enabled Oxidation of Gold(I) Complexes with *o*-Quinones. *Chem. Sci.* **2022**, *13*, 10499–10505.

(30) Cadge, J. A.; Bower, J. F.; Russell, C. A. A Systematic Study of the Effects of Complex Structure on Aryl Iodide Oxidative Addition at Bipyridyl-Ligated Gold(I) Centers. *Angew. Chem. Int. Ed.* **2021**, *60*, 24976–24983.

(31) Lee, Y. H.; Morandi, B. Transition Metal-Mediated Metathesis between P–C and M–C Bonds: Beyond a Side Reaction. *Coord. Chem. Rev.* **2019**, *386*, 96–118.

(32) Tamaki, A.; Magennis, S. A.; Kochi, J. K. Catalysis by Gold. Alkyl Isomerization, *Cis-Trans* Rearrangement, and Reductive Elimination of Alkylgold(III) Complexes. *J. Am. Chem. Soc.* **1974**, *96*, 6140–6148.

(33) Komiya, S.; Albright, T. A.; Hoffmann, R.; Kochi, J. K. Reductive Elimination and Isomerization of Organogold Complexes. Theoretical Studies of Trialkylgold Species as Reactive Intermediates. *J. Am. Chem. Soc.* **1976**, *98*, 7255–7265.

(34) Kuch, P. L.; Tobias, R. S. Synthesis of Cationic Dialkylgold(III) Complexes: Nature of the Facile Reductive Elimination of Alkane. *J. Organomet. Chem.* **1976**, *122*, 429–446.

(35) Mankad, N. P.; Toste, F. D. C–C Coupling Reactivity of an Alkylgold(III) Fluoride Complex with Arylboronic Acids. *J. Am. Chem. Soc.* **2010**, *132*, 12859–12861.

(36) Komiya, S.; Kochi, J. K. Electrophilic Cleavage of Organogold Complexes with Acids. The Mechanism of the Reductive Elimination of Dialkyl(aniono)gold(III) Species. *J. Am. Chem. Soc.* **1976**, *98*, 7599–7607.

(37) Komiya, S.; Ozaki, S.; Shibue, A. Leaving Group Selectivity in Reductive Elimination from Organogold(III) Complexes. *J. Chem. Soc., Chem. Commun.* **1986**, 1555–1556.

(38) Winston, M. S.; Wolf, W. J.; Toste, F. D. Halide-Dependent Mechanisms of Reductive Elimination from Gold(III). *J. Am. Chem. Soc.* **2015**, *137*, 7921–7928.

(39) Levin, M. D.; Toste, F. D. Gold-Catalyzed Allylation of Aryl Boronic Acids: Accessing Cross-Coupling Reactivity with Gold. *Angew. Chem. Int. Ed.* **2014**, *53*, 6211–6215.

(40) Genoux, A.; González, J. A.; Merino, E.; Nevado, C. Mechanistic Insights into $C(sp^2)$–C(sp)N Reductive Elimination from Gold(III) Cyanide Complexes. *Angew. Chem. Int. Ed.* **2020**, *59*, 17881–17886.

(41) Liu, S.; Kang, K.; Liu, S.; Wang, D.; Wei, P.; Lan, Y.; Shen, Q. The Difluoromethylated Organogold(III) Complex *cis*-[$Au(PCy_3)(4\text{-}F\text{-}C_6H_4)(CF_2H)(Cl)$]: Preparation, Characterization, and Its $C(sp^2)$–CF_2H Reductive Elimination. *Organometallics* **2018**, *37*, 3901–3908.

(42) Rocchigiani, L.; Fernandez-Cestau, J.; Budzelaar, P. H. M.; Bochmann, M. Reductive Elimination Leading to C–C Bond Formation in Gold(III) Complexes: A Mechanistic and Computational Study. *Chem. Eur. J.* **2018**, *24*, 8893–8903.

(43) Vicente, J.; Bermúdez, M. D.; Escribano, J. Gold in Organic Synthesis. Preparation of Symmetrical and Unsymmetrical Biaryls via Carbon-Carbon Coupling from *cis*-Diarylgold(III) Complexes. *Organometallics* **1991**, *10*, 3380–3384.

(44) Vicente, J.; Bermúdez, M. D.; Escribano, J.; Carrillo, M. P.; Jones, P. G. Synthesis of Intermediates in the C–H Activation of Acetone with 2-Phenylazophenylgold(III)

Complexes and in the C–C Coupling of Aryl Groups from Diarylgold(III) Complexes. Crystal and Molecular Structures of [Au{C_6H_3(NNC_6H_4Me-4′)-2-Me-5}(acac-*C*)Cl] (acac = acetylacetonate), *cis*-[Au(C_6H_4NNPh-2)Cl_2(PPh_3)], and [Au($C_6H_4CH_2NMe_2$-2)(C_6F_5)Cl]. *J. Chem. Soc., Dalton Trans.* **1990**, 3083–3089.

(45) Kang, K.; Liu, S.; Xu, T.; Wang, D.; Leng, X.; Bai, R.; Lan, Y.; Shen, Q. $C(sp^2)$–$C(sp^2)$ Reductive Elimination from Well-Defined Diarylgold(III) Complexes. *Organometallics* **2017**, *36*, 4727–4740.

(46) Wolf, W. J.; Winslow, M. S.; Toste, F. D. Exceptionally Fast Carbon–Carbon Bond Reductive from Gold(III). *Nat. Chem.* **2014**, *6*, 159–164.

(47) Harper, M. J.; Arthur, C. J.; Crosby, J.; Emmett, E. J.; Falconer, R. L.; Fensham-Smith, A. J.; Gates, P. J.; Leman, T.; McGrady, J. E.; Bower, J. F.; Russell, C. A. Oxidative Addition, Transmetalation, and Reductive Elimination at a 2,2′-Bipyridyl-Ligated Gold Center. *J. Am. Chem. Soc.* **2018**, *140*, 4440–4445.

(48) Bonsignore, R.; Thomas, S. R.; Rigoulet, M.; Jandl, C.; Pöthig, A.; Bourissou, D.; Barone, G.; Casini, A. C–C Cross-Couplings from a Cyclometalated Au(III) C^N Complex: Mechanistic Insights and Synthetic Developments. *Chem. Eur. J.* **2021**, *27*, 14322–14334.

(49) Mankad, N. P.; Toste, F. D. $C(sp^3)$–F Reductive Elimination from Alkylgold(III) Fluoride Complexes. *Chem. Sci.* **2012**, *3*, 72–76.

(50) Scott, V. J.; Labinger, J. A.; Bercaw, J. E. Mechanism of Reductive Elimination of Methyl Iodide from a Novel Gold(III)–Monomethyl Complex. *Organometallics* **2010**, *29*, 4090–4096.

(51) Ghidiu, M. J.; Pistner, A. J.; Yap, G. P. A.; Lutterman, D. A.; Rosenthal, J. Thermal versus Photochemical Reductive Elimination of Aryl Chlorides from NHC–Gold Complexes. *Organometallics* **2013**, *32*, 5026–5029.

(52) Blaya, M.; Bautista, D.; Gil-Rubio, J.; Vicente, J. Synthesis of Au(I) Trifluoromethyl Complexes. Oxidation to Au(III) and Reductive Elimination of Halotrifluoromethanes. *Organometallics* **2014**, *33*, 6358–6368.

(53) Kim, J. H.; Mertens, R. T.; Agarwal, A.; Parkin, S.; Berger, G.; Awuah, S. G. Direct Intramolecular Carbon(sp^2)–Nitrogen(sp^2) Reductive Elimination from Gold(III). *Dalton Trans*. **2019**, *48*, 6273–6282.

(54) Serra, J.; Parella, T.; Ribas, X. Au(III)-Aryl Intermediates in Oxidant-Free C–N and C–O Cross-Coupling Catalysis. *Chem. Sci*. **2017**, *8*, 946–952.

(55) Serra, J.; Whiteoak, C. J.; Acuña-Parés, F.; Font, M.; Luis, J. M.; Lloret-Fillol, J.; Ribas, X. Oxidant-Free Au(I)-Catalyzed Halide Exchange and Csp^2–O Bond Forming Reactions. *J. Am. Chem. Soc*. **2015**, *137*, 13389–13397.

(56) Currie, L.; Rocchigiani, L.; Hughes, D. L.; Bochmann, M. Carbon–Sulfur Bond Formation by Reductive Elimination of Gold(III) Thiolates. *Dalton Trans*. **2018**, *47*, 6333–6343.

(57) Kawai, H.; Wolf, W. J.; DiPasquale, A. G.; Winston, M. S.; Toste, F. D. Phosphonium Formation by Facile Carbon–Phosphorus Reductive Elimination from Gold(III). *J. Am. Chem. Soc*. **2016**, *138*, 587–593.

(58) Bonsignore, R.; Thomas, S. R.; Klooster, W. T.; Coles, S. J.; Jenkins, R. L.; Bourissou, D.; Barone, G.; Casini, A. Carbon–Phosphorus Coupling from C^N Cyclometalated Au^{III}

Complexes. *Chem. Eur. J.* **2020**, *26*, 4226–4231.

(59) Kang, K.; Liu, S.; Xu, C.; Lu, Z.; Liu, S.; Leng, X.; Lan, Y.; Shen, Q. C(sp^2)–X (X = Cl, Br, and I) Reductive Eliminations from Well-Defined Gold(III) Complexes: Concerted or Dissociation Pathways? *Organometallics* **2021**, *40*, 2231–2239.

(60) Howells, R. D.; Mc Cown, J. D. Trifluoromethanesulfonic Acid and Derivatives. *Chem. Rev.* **1977**, *77*, 69–92.

(61) Baum, K.; Beard, C. D. Reactions of Dichlorine Heptoxide with Alcohols. *J. Am. Chem. Soc.* **1974**, *96*, 3233–3237.

(62) Zefirov, N. S.; Koz'min, A. S.; Zhdankin, V. V.; Kirin, V. N.; Yur'eva, N. M.; Sorokin, V. D. Competitive Binding of Super-Weak Nucleophiles in Carbocationic-Like Processes. *Chem. Scr.* **1983**, *22*, 195–200.

(63) Traversa, E.; Templeton, J. L.; Cheng, H. Y.; Mohadjer Beromi, M.; White, P. S.; West, N. M. Reductive Elimination from Platinum(IV) Aminotroponiminate Dimethyl Complexes Promoted by Sterically Hindered Lewis Bases. *Organometallics* **2013**, *32*, 1938–1950.

(64) Jimenez, M. V.; Sola, E.; Egea, M. A.; Huet, A.; Francisco, A. C.; Lahoz, F. J.; Oro, L. A. Key Factors Determining the Coarse of Methyl Iodide Oxidative Addition to Diamidonaphthalene-Bridged Diiridium(I) and Dirhodium(I) Complexes. *Inorg. Chem.* **2000**, *39*, 4868–4878.

(65) Grotjahn, D. B.; Gong, Y.; Zakharov, L.; Golen, J. A.; Rheingold, A. L. Changes in Coordination of Sterically Demanding Hybrid Imidazolylphosphine Ligands on Pd(0) and

Pd(II). *J. Am. Chem. Soc.* **2006**, *128*, 438–453.

(66) Hill, G. S.; Yap, G. P. A.; Puddephatt, R. J. Electrophilic Platinum Complexes: Methyl Transfer Reactions and Catalytic Reductive Elimination of Ethane from a Tetramethylplatinum(IV) Complex. *Organometallics* **1999**, *18*, 1408–1418.

(67) Johnson, M. T.; Janse Van Rensburg, J. M.; Axelsson, M.; Ahlquist, M. S. G.; Wendt, O. F. Reactivity of NHC Au(I)-C σ-Bonds with Electrophiles. An Investigation of Their Possible Involvement in Catalytic C-C Bond Formation. *Chem. Sci.* **2011**, *2*, 2373–2377.

(68) Suero, M. G.; Bayle, E. D.; Collins, B. S. L.; Gaunt, M. J. Copper-Catalyzed Electrophilic Carbofunctionalization of Alkynes to Highly Functionalized Tetrasubstituted Alkenes. *J. Am. Chem. Soc.* **2013**, *135*, 5332–5335.

(69) Planas, O.; Peciukenas, V.; Cornella, J. Bismuth-Catalyzed Oxidative Coupling of Arylboronic Acids with Triflate and Nonaflate Salts. *J. Am. Chem. Soc.* **2020**, *142*, 11382–11387.

(70) Levin, M. D.; Chen, T. Q.; Neubig, M. E.; Hong, C. M.; Theulier, C. A.; Kobylianskii, I. J.; Janabi, M.; O'Neil, J. P.; Toste, F. D. A Catalytic Fluoride-Rebound Mechanism for $C(sp^3)$-CF_3 Bond Formation. *Science* **2017**, *356*, 1272–1276.

(71) Camasso, N. M.; Pérez-Temprano, M. H.; Sanford, M. S. $C(sp^3)$–O Bond-Forming Reductive Elimination from Pd^{IV} with Diverse Oxygen Nucleophiles. *J. Am. Chem. Soc.* **2014**, *136*, 12771–12775.

(72) Roth, K. E.; Blum, S. A. Relative Kinetic Basicities of Organogold Compounds. *Organometallics* **2010**, *29*, 1712–1716.

(73) Kütt, A.; Selberg, S.; Kaljurand, I.; Tshepelevitsh, S.; Heering, A.; Darnell, A.; Kaupmees, K.; Piirsalu, M.; Leito, I. PKa Values in Organic Chemistry – Making Maximum Use of the Available Data. *Tetrahedron Lett*. **2018**, *59*, 3738–3748.

(74) Komiya, S.; Albright, T. A.; Hoffmann, R.; Kochi, J. K. The Stability of Organogold Compounds. Hydrolytic, Thermal, and Oxidative Cleavages of Dimethylaurate(I) and Tetramethylaurate(III). *J. Am. Chem. Soc*. **1977**, *99*, 8440–8447.

(75) Fan, D.; Meléndez, E.; Ranford, J. D.; Lee, P. F.; Vittal, J. J. Study on Carbon–Hydrogen Activation of Ketones by Gold(III) Complexes and the Synthesis and Characterization of Two Ketonylgold(III) Complexes. *J. Organomet. Chem*. **2004**, *689*, 2969–2974.

(76) Pérez-Bitrián, A.; Alvarez, S.; Baya, M.; Echeverría, J.; Martín, A.; Orduna, J.; Menjón, B. Terminal Au–N and Au–O Units in Organometallic Frames. *Chem. Eur. J*. **2022**, *accepted article*, https://doi.org/https://doi.org/10.1002/chem.202203181.

(77) Ellwanger, M. A.; Steinhauer, S.; Golz, P.; Beckers, H.; Wiesner, A.; Braun-Cula, B.; Braun, T.; Riedel, S. Taming the High Reactivity of Gold(III) Fluoride: Fluorido Gold(III) Complexes with N-Based Ligands. *Chem. Eur. J*. **2017**, *23*, 13501–13509.

(78) Kumar, R.; Linden, A.; Nevado, C. Evidence for Direct Transmetalation of Au^{III}-F with Boronic Acids. *J. Am. Chem. Soc*. **2016**, *138*, 13790–13793.

(79) Komiya, S.; Shibue, A. Steric and Electronic Effects of the Tertiary Phosphine Ligand on the Dissociative Reductive Elimination from *cis*-Aryldimethyl(triarylphosphine)gold(III). *Organometallics* **1985**, *4*, 684–687.

(80) O'Reilly, M. E.; Pahls, D. R.; Webb, J. R.; Boaz, N. C.; Majumdar, S.; Hoff, C. D.;

Groves, J. T.; Cundari, T. R.; Gunnoe, T. B. Reductive Functionalization of a Rhodium(III)-Methyl Bond by Electronic Modification of the Supporting Ligand. *Dalton Trans*. **2014**, *43*, 8273–8281.

(81) Feller, M.; Diskin-Posner, Y.; Leitus, G.; Shimon, L. J. W.; Milstein, D. Direct Observation of Reductive Elimination of MeX (X = Cl, Br, I) from Rh^{III} Complexes: Mechanistic Insight and the Importance of Sterics. *J. Am. Chem. Soc*. **2013**, *135*, 11040–11047.

(82) Marquard, S. L.; Hartwig, J. F. C(sp^3)-O Bond-Forming Reductive Elimination of Ethers from Bisphosphine-Ligated Benzylpalladium(II) Aryloxide Complexes. *Angew. Chem. Int. Ed*. **2011**, *50*, 7119–7123.

(83) Pérez-Temprano, M. H.; Racowski, J. M.; Kampf, J. W.; Sanford, M. S. Competition between sp^3-C–N *vs* sp^3-C–F Reductive Elimination from Pd^{IV} Complexes. *J. Am. Chem. Soc*. **2014**, *136*, 4097–4100.

(84) Park, H.; Verma, P.; Hong, K.; Yu, J. Q. Controlling Pd(IV) Reductive Elimination Pathways Enables Pd(II)-Catalysed Enantioselective C(sp^3)-H Fluorination. *Nat. Chem*. **2018**, *10*, 755–762.

(85) Luinstra, G. A.; Labinger, J. A.; Bercaw, J. E. Mechanism and Stereochemistry for Nucleophilic Attack at Carbon of Platinum(IV) Alkyls: Model Reactions for Hydrocarbon Oxidation with Aqueous Platinum Chlorides. *J. Am. Chem. Soc*. **1993**, *115*, 3004–3005.

(86) Williams, B. S.; Goldberg, K. I. Studies of Reductive Elimination Reactions To Form Carbon–Oxygen Bonds from Pt(IV) Complexes. *J. Am. Chem. Soc*. **2001**, *123*, 2576–

2587.

(87) Pawlikowski, A. V; Getty, A. D.; Goldberg, K. I. Alkyl Carbon-Nitrogen Reductive Elimination from Platinum(IV)-Sulfonamide Complexes. *J. Am. Chem. Soc.* **2007**, *129*, 10382–10393.

(88) Rivada-Wheelaghan, O.; Roselló-Merino, M.; Díez, J.; Maya, C.; López-Serrano, J.; Conejero, S. Formation of C-X Bonds through Stable Low-Electron-Count Cationic Platinum(IV) Alkyl Complexes Stabilized by N-Heterocyclic Carbenes. *Organometallics* **2014**, *33*, 5944–5947.

(89) Dhakal, B.; Bohé, L.; Crich, D. Trifluoromethanesulfonate Anion as Nucleophile in Organic Chemistry. *J. Org. Chem.* **2017**, *82*, 9263–9269.

(90) Jones, C. J.; Taube, D.; Ziatdinov, V. R.; Periana, R. A.; Nielsen, R. J.; Oxgaard, J.; Goddard III, W. A. Selective Oxidation of Methane to Methanol Catalyzed, with C–H Activation, by Homogeneous, Cationic Gold. *Angew. Chem. Int. Ed.* **2004**, *43*, 4626–4629.

For Table of Contents Only

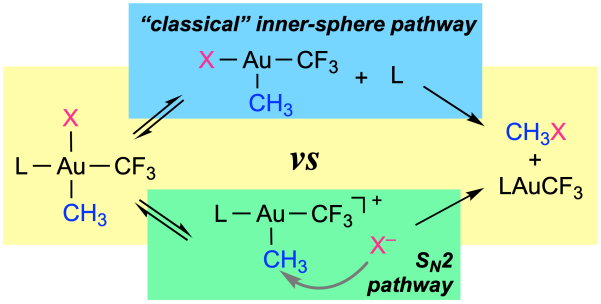

The first experimental and computational evidence of a S_N2 mechanism for the reductive elimination reaction from Au(III) complexes is reported. Very rare eliminations of highly electrophilic molecules such as MeOTf or $MeOClO_3$ are demonstrated